Accepted Manuscript

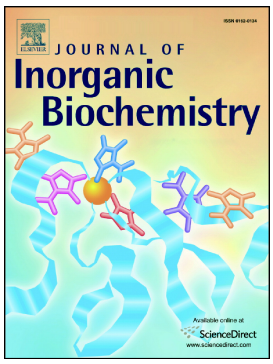

Mass spectrometric studies of Cu(I)-binding to the N-terminal domains of B. subtilis CopA and influence of bacillithiol

Kristine L. Kay, Chris J. Hamilton, Nick E. Le Brun

PII: S0162-0134(18)30430-6
DOI: doi:10.1016/j.jinorgbio.2018.10.004
Reference: JIB 10578

To appear in: *Journal of Inorganic Biochemistry*

Received date: 18 July 2018
Revised date: 11 October 2018
Accepted date: 12 October 2018

Please cite this article as: Kristine L. Kay, Chris J. Hamilton, Nick E. Le Brun , Mass spectrometric studies of Cu(I)-binding to the N-terminal domains of B. subtilis CopA and influence of bacillithiol. Jib (2018), doi:10.1016/j.jinorgbio.2018.10.004

Mass spectrometric studies of Cu(I)-binding to the N-terminal domains of *B. subtilis* CopA and influence of bacillithiol

Kristine L. Kay[1], Chris J. Hamilton[2] and Nick E. Le Brun[1]*

[1]Centre for Molecular and Structural Biochemistry, School of Chemistry, University of East Anglia, Norwich Research Park, Norwich NR4 7TJ, UK

[2]School of Pharmacy, University of East Anglia, Norwich Research Park, Norwich NR4 7TJ, UK

*Address correspondence to: Nick E Le Brun, School of Chemistry, University of East Anglia, Norwich NR4 7TJ, UK. Tel. +44 1603 592699; Fax. +44 1603 592003; Email: n.le-brun@uea.ac.uk

Graphical abstract

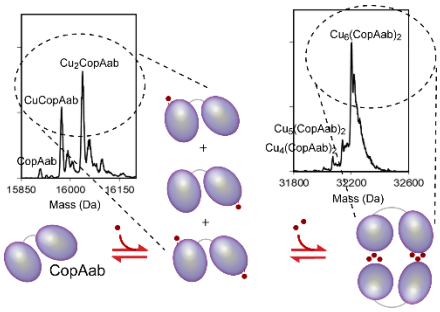

Synopsis. CopA is a Cu(I)-exporting transmembrane P_{1B}-type ATPase from *Bacillus subtilis.* Electrospray ionization mass spectrometric analysis of Cu(I)-binding to the N-terminal domains of CopA (CopAab) reveals formation of a dimeric form, $Cu_6(CopAab)_2$, at > 1 Cu(I)/protein. Dimeric forms persist in the presence of bacillithiol.

Highlights

- CopA is a Cu(I)-exporting transmembrane P_{1B}-type ATPase from *Bacillus subtilis*
- ESI-MS studies of the N-terminal domains of CopA (CopAab) reveals copper-bound forms
- At low copper (up to 1 per protein), singly and doubly Cu(I)-bound forms predominate
- At higher copper (> 1 per protein), dimeric CopAab containing six Cu(I) predominate
- Dimeric CopAab persists in the presence of bacillithiol at physiological ratios

Keywords: Copper trafficking, electrospray ionisation mass spectrometry, *Bacillus subtilis*, copper-mediated association, bacillithiol

ABSTRACT

CopA is a Cu(I)-exporting transmembrane P_{1B}-type ATPase from *Bacillus subtilis*. It contains two N-terminal cytoplasmic domains, CopAab, which bind Cu(I) with high affinity and to form higher-order complexes with multiple Cu(I) ions. To determine the precise nature of these species, electrospray ionization mass spectrometry (ESI-MS) under non-denaturing conditions was employed. Up to 1 Cu per CopAab resulted in Cu coordination to one or both CopAab domains. At > 1 Cu/CopAab, two distinct dimeric charge state envelopes were observed, corresponding to distinct conformations, each with $Cu_6(CopAab)_2$ as its major form. The influence of the physiologically relevant low molecular weight thiol bacillithiol (BSH) on Cu(I)-binding to CopAab was assessed. Dimeric CopAab persisted in the presence of BSH, with previously undetected $Cu_7(CopAab)_2$ and $Cu_6(CopAab)_2(BSH)$ forms apparent.

Introduction

Copper is an essential metal transported by dedicated copper chaperone proteins that deliver it to copper-requiring enzymes and detoxify it when in excess [1]. The latter process, which involves copper export across the cytoplasmic membrane, is essential to cell survival due to the potentially toxic nature of elevated cellular copper levels. Translocation of Cu(I) across the *Bacillus subtilis* cell membrane takes place via the integral membrane P-type ATPase, CopA [2, 3].

P-type ATPase protein family members typically contain a central core of transmembrane helices, an actuator domain (A-domain) and an ATP-binding domain (ATP-BD), comprising two distinct sub-domains involved in nucleotide-binding (N) and phosphorylation (P) [4]. The P-type ATPases are further divided into subclasses based upon several structural features [5]. The P_{1B}-type ATPases contain an additional two helices in the transmembrane core, and are also distinguished by possession of a Cys-Pro-Cys (CPC) transmembrane metal-binding motif located in helix 4, and one or more soluble cytoplasmic domains (MBDs) at the N- and, sometimes, C-termini. The two N-terminal cytoplasmic MBDs in *B. sutbilis* CopA, CopAab, possess the same βαββαβ fold as that of the *B. subtilis* Atx1 (antioxidant protein 1, a eukaryotic copper chaperone)-like metallochaperone CopZ. Each individual domain, CopAa and CopAb, contains a conserved MXCXXC copper-binding motif with two solvent-exposed cysteines located between the end of the first loop and the beginning of the first α-helix [6].

The exact role of MBDs in ATPase function is unclear. It has been proposed that, in some cases, they are required for copper transfer activity [7, 8], but in others it has been shown that they are not [9], and available structural data indicate that they are too remote from the transmembrane transport site to be directly involved. However, protein-protein interaction and protein phosphorylation studies, together with their proximity to the actuator and nucleotide-binding domains, have led to a model in which the MBDs perform a regulatory role through interactions with these domains that modulates not only Cu(I) transport activity but (in eukaryotes) also trafficking between sub-cellular locations [10-13].

Cu(I) binding to the MBDs of CopA, both as isolated domains (CopAa and CopAb) [14, 15] and as a two domain protein, CopAab [16], has been characterised previously using spectroscopic and bioanalytical techniques. Initial binding of Cu(I) to CopAab occurs with high affinity ($K \approx 4 \times 10^{17}$ M^{-1}) [17], and CopAab was shown to undergo Cu(I)-mediated dimerization above 1 Cu/protein. Data from AUC and SEC suggested that a small portion of dimer (≈ 5%) was present at 1 Cu/protein and by 2 Cu/protein the association state was fully dimeric [16]. Dimeric CopAab was also shown to be capable of accommodating multiple Cu(I) ions. Copper binding by CopAab at a ratio of 2 Cu/protein resulted in a highly luminescent species, predicted to be due to a $Cu_4(CopAab)_2$ form [17]. However, luminescence quenching beyond a ratio of 2:1 suggested that dimeric CopAab may be able to bind additional Cu(I) ions [17]. Recent studies of a 1:1 mixture of separate CopAa and CopAb showed that the domains do not form a stable complex in the absence of a covalent linker, though there was evidence of a weak interaction between them [18].

The regulation of cellular Cu(I) levels could be influenced by cytoplasmic low molecular weight thiol-containing species. For example, glutathione may serve as a copper-binding intermediate between the eukaryotic importer Ctr1 (high affinity copper transporter 1) and cytoplasmic chaperones [19]. A role in metal trafficking has also been suggested for bacillithiol (BSH), the cytoplasmic low molecular weight thiol of *B. subtilis*, and related species [20-22]. BSH has been shown to detoxify xenobiotic compounds and antibiotics and serve a protective effect against cysteine oxidation through protein S-bacillithiolation [20, 21]. Cu(I)-induced *copZA* induction was elevated in BSH-null mutants of *B. subtilis*, suggesting the absence of BSH led to elevated labile Cu(I) levels and the presence of BSH plays a role in Cu(I) buffering. Recent studies of Cu(I)-binding to *B. subtilis* CopZ using electrospray ionisation mass spectrometry (ESI-MS) under non-denaturing conditions, in the absence and presence of BSH, revealed bacillithiolation and a range of BSH adducts of CopZ in which the thiol most likely serves as an exogenous Cu(I) ligand [22]. Low molecular weight thiols have previously been shown to influence CopAab association state behaviour [17], but the effects of BSH have not been investigated.

Despite the previous characterisation of complex Cu(I) binding to CopAab, the precise nature of species and mixtures of species which form as Cu(I) levels vary is unknown. The recent investigation of Cu(I)-binding to CopZ using ESI-MS revealed precise information about the nature of Cu(I)-CopZ species, suggesting that similar high resolution information about CopAab could be available. Thus, non-denaturing ESI-MS studies of Cu(I)-binding to CopAab, in the absence and presence of BSH, were carried out. The data are consistent with solution spectroscopic and bioanalytical studies, demonstrating Cu(I)-mediated dimerization of CopAab, and the formation of a $Cu_6(CopAab)_2$ form at high copper loadings. While the non-physiological thiol dithiothreitol (DTT) severely inhibited dimerization of CopAab, BSH, at ratios to CopAab of 1-10, was found to promote dimerization and to influence the distribution of Cu(I)-bound species. In contrast to CopZ [22], bacillithiolation and BSH-adduct formation were not readily detected.

Materials and methods

Purification of CopAab. Overexpression and purification of CopAab was carried out as previously described [16], except for the inclusion of an additional step to remove contaminating nucleic acids following ion exchange chromatography. $(NH_4)_2SO_4$ was added to fractions containing CopAab (determined by SDS-PAGE analysis), to a final concentration of 3 M. The protein solution was then loaded onto a 15 mL phenyl-sepharose hydrophobic interaction chromatography (HIC) column (GE Healthcare), previously equilibrated with 5 CV 100 mM HEPES, 100 mM NaCl, 3 M $(NH_4)_2SO_4$, 15 mM DTT, pH 7.0. The column was washed with 20 CV binding buffer before applying a 100 mL gradient of 3 – 0 M $(NH_4)_2SO_4$. Fractions containing CopAab (as determined by SDS-PAGE analysis) were buffer exchanged into 100 mM HEPES, 100 mM NaCl, pH 7.0 and concentrated to < 2.5 mL, using a centrifugal ultrafiltration unit (Vivaspin; Millipore) at 8000 × g and 4 °C. The protein solution was passed through a 0.45 µm filter (Sartorius) and DTT added to a final concentration of 15 mM before applying to the Sephacryl S-100 gel filtration column. Subsequent purification steps were carried out as previously described [16].

Mass spectrometry. ESI-MS samples of CopAab were prepared by first adding 15 mM DTT (Formedium) and removing excess reductant by passage down a G25 Sephadex column (PD10, GE Healthcare) in an anaerobic glovebox (Faircrest Engineering, O_2 concentration < 2 ppm) using 20 mM ammonium acetate (Sigma), pH 7.4, as the elution buffer. Protein concentrations were calculated using an extinction coefficient, $\varepsilon_{276\ nm}$, of 5800 M^{-1} cm^{-1} [17], before anaerobic addition of Cu(I) using a microsyringe (Hamilton). UV-visible absorbance spectra were recorded on a Jasco V-550 spectrophotometer. To prepare Cu(I)-bound CopAab samples, a deoxygenated solution of Cu(I)Cl prepared in 100 mM HCl (Sigma), 1 M NaCl was added to anaerobic, reduced CopAab using a microsyringe (Hamilton) in an anaerobic glovebox. Unbound Cu(I) was removed by passage of the sample down a G25 Sephadex column (PD10, GE Healthcare) equilibrated with 20 mM ammonium acetate, pH 7.4. The protein sample was diluted with 20 mM ammonium acetate to a working sample concentration of 5 µM. Thiol experiments were carried out using dithiothreitol (DTT) (Formedium) or BSH (synthesised as described previously [23]) and prepared anaerobically using deoxygenated LC-MS grade water (HiPerSolv, VWR). Solutions of CopAab were prepared at 4.0 Cu(I)/protein (as described above), where thiol solution was added to yield ratios of 1, 5, 10, or 25 thiol per protein. Mass spectra were acquired using a Bruker micrOTOF-QIII electrospray ionisation (ESI) time-of-flight (TOF) mass spectrometer (Bruker Daltonics, Coventry, UK), in positive ion mode. The ESI-TOF was calibrated using ESI-L Low Concentration Tuning Mix (Agilent Technologies, San Diego, CA). Native protein samples were introduced to the ESI source at 4 °C via a syringe pump (Cole-Parmer) at 5 mL/min, and data acquired for 2 min, with ions scanned between 500 – 3000 m/z. MS acquisition was controlled using Bruker oTOF Control software, with parameters as follows: dry gas flow 5 L/min, nebuliser gas pressure 0.8 Bar, dry gas 180 °C, capillary voltage 4500 V, offset 500 V, isCID (in-source collision induced dissociation) energy 0 eV, quadrupole radio frequency (RF) stepping set at 2000 Vpp (peak to peak volts; 25%) and 3200 Vpp (75%). Processing and analysis of MS experimental data were carried out using Compass DataAnalysis version 4.1 (Bruker Daltonik,

Bremen, Germany). The spectra were deconvoluted using the ESI Compass version 1.3 Maximum Entropy deconvolution algorithm over a mass range of 15000 – 35000 Da. Exact masses were determined from peak centroids, with 3-point Gaussian smoothing applied only to spectra acquired in the presence of BSH. Predicted masses are given as the isotope average of the neutral protein or protein complex, in which Cu(I)-binding is expected to be charge compensated For ions due to CopAab-Cu species, m/z values corresponded to $[M + x(Cu) + (n-x)H]^{n+}/n$, where M is the molecular mass of the protein and x the number of coordinated Cu^{+} ions, which offsets the number of protons required to achieve the observed charge state (n+) [22, 24].

Results and Discussion

ESI-MS studies reveal Cu(I)-mediated dimerization of CopAab and formation of $Cu_6(CopAab)_2$

ESI-MS under non-denaturing conditions preserves protein structure and non-covalent protein-metal and protein-protein interactions, and can provide high resolution information about the species present in complex mixtures [24, 25]. The m/z mass spectra for CopAab containing 0.5, 1.0, 2.0 and 4.0 Cu/protein are presented in Fig. 1. Three charge state envelopes were observed, corresponding to monomeric (+8, +9) and dimeric (+11 – +14; and +16 – +18) forms of CopAab. At 0.5 and 1.0 Cu/CopAab (Fig. 1A and B, respectively), the monomer charge envelope (8+, 9+) was predominant, with no significant intensity due to dimeric charge states. The dimer charge states increased in intensity at higher levels of copper, such that they matched or exceeded the monomeric charge state envelope in intensity at a level of 4.0 Cu/CopAab (Fig. 1C and D).

Deconvoluted mass spectra in the monomer and dimer regions are shown on the right of Fig. 1. These illustrate that CuCopAab and Cu_2CopAab (see Table 1 for observed and predicted masses) were the most abundant species at 0.5 and 1.0 Cu/CopAab (Fig. 1A and B); here copper is bound at one or both of the copper-binding domains (CopAa and/or CopAb). The relative intensity of Cu_2CopAab increased to become the dominant copper-bound peak at 2.0 Cu/protein. The structure of *B. subtilis* CopAab revealed that the two copper-binding motifs are remote from one another and

cannot participate in binding the same Cu(I) ion [16]. NMR data also established that CopZ interacts with, and can deliver Cu(I) to, both CopAab domains with no observable preference [16, 26]. Although the ESI-MS data cannot determine which domain is bound to Cu(I), the data are consistent with binding occurring to both domains without preference, such that a mixture of apo, singly and doubly Cu(I)-bound CopAab species was observed at lower copper levels.

At 2 Cu/CopAab, peaks were also observed in the dimer region, with the major peak corresponding to $Cu_6(CopAab)_2$, with much smaller peaks due to $Cu_5(CopAab)_2$ and $Cu_4(CopAab)_2$ (Fig. 1C). A very similar pattern but with greater relative abundance in the dimer region (such that it was greater than that of the monomer region) was observed at 4 Cu/CopAab (Fig. 1D). The consistently low intensity of $Cu_4(CopAab)_2$ and $Cu_5(CopAab)_2$ peaks and the lack of other higher order Cu(I)-bound forms suggest that $Cu_6(CopAab)_2$ represents a particularly stable form of dimeric CopAab. Relative abundances of species (mean values over n = 3) are shown in Fig. S1.

The ESI-MS data are consistent with previous solution spectroscopic studies demonstrating complex copper-binding behaviour of CopAab, with Cu(I)-mediated dimerisation occurring above a level of 1 Cu/protein. We might have expected the protein to be fully dimeric at 2 Cu/CopAab. In reality, some monomeric species remained, even at the highest level of copper. However, the observation of monomer forms of dimeric species is a common observation by ESI-MS, where the monomer-monomer interactions do not quantitatively survive the ionisation process [24, 27].

Previous spectroscopic studies demonstrated the formation of a luminescent species that is characteristic of a solvent excluded multi-nuclear Cu(I) centre [17]. This was observed to maximise at ~2 Cu/protein before losing intensity as further copper was added [16, 17]. From this, a model was proposed in which a $Cu_4(CopAab)_2$ species forms initially upon CopAab dimerization, followed by $Cu_5(CopAab)_2$ and $Cu_6(CopAab)_2$ species as further copper is added, with $Cu_7(CopAab)_2$ and $Cu_8(CopAab)_2$ forms predicted to be the end point of the Cu(I) titration [17]. The ESI-MS data are broadly in agreement with this, with $Cu_4(CopAab)_2$, $Cu_5(CopAab)_2$ and $Cu_6(CopAab)_2$ species detected. It was anticipated that the $Cu_4(CopAab)_2$ form would be dominant at 2 Cu/CopAab, but

this was not apparent from the ESI-MS data. This could be a result of the tendency of the CopAab dimer to dissociate during ionisation, with loss of some Cu(I) that may be readily picked up by remaining dimeric CopAab species. However, the data clearly indicate that the $Cu_6(CopAab)_2$ form is highly stable, and that higher order Cu(I)-bound species are not readily formed. Thus, the ESI-MS data provide, for the first time, evidence of the precise nature of the Cu(I)-species formed.

The presence of two distinct dimeric species in the m/z spectra of CopAab containing 2 or greater Cu/CopAab (charge states 11+, 12+, 13+, 14+ and 16+, 17+, 18+, respectively; Fig. 1) indicated the presence of two distinct forms of dimeric CopAab (principally $Cu_6(CopAab)_2$). These most likely correspond to two conformations, with the species giving rise to the higher charge states most likely adopting a more open structure that permits a greater extent of protonation. These observations could be related to previous studies of CopAab by far UV-CD, which showed that higher copper loadings resulted in loss of CopAab secondary structure, most likely resulting from partial unfolding and leading to significant conformational rearrangement [16].

The detection of CopAab as a dimer at higher Cu loading implies that the full length protein, CopA, could undergo dimerization in response to Cu status under some conditions. While there is no *in vivo* data for CopA that supports this possibility, we note that metal ion transporting P-type ATPases have been reported to dimerize (eg [28]) and, more importantly, the Wilson's disease protein, ATP7B, was recently shown to form stable dimers *in vitro* and in cells [29]. Deletion of the first four (of the six) N-terminal metal-binding domains did not disrupt dimerization, indicating that the dimer interface is formed by the domains that are conserved amongst Cu(I)-transporting P-type ATPases.

ESI-MS studies reveal distinct effects of DTT and BSH on association state and Cu(I)-binding properties of CopAab

The cellular cytosol is abundant in low molecular weight thiols that are capable of binding Cu(I) [30] and can potentially impact copper trafficking [31, 32]. Previous AUC experiments conducted with

CopAab at elevated Cu(I) levels in the presence of 20-fold excess of DTT illustrated that this thiol prevented protein dimerization, with glutathione and cysteine having a less severe effect [16]. These studies pre-dated the discovery of bacillithiol as a major cytoplasmic thiol in *B. subtilis* [33]. Therefore the influence of DTT and BSH on the speciation of CopAab at 4 Cu(I) per protein was examined using ESI-MS at thiol to protein ratios of 1, 5, 10 and 25 for both DTT and BSH. The m/z spectra for CopAab in the presence of DTT (Fig. S2) featured fewer peaks than the equivalent thiol-free spectrum (Fig. 1D), comprising mostly monomeric species (+8, +9) with the more compact dimeric copper-bound form (+12, +13) corresponding to $Cu_6(CopAab)_2$ initially present at low abundance, but this was lost at ratios of DTT > 1. The less compact, higher dimeric charge states were entirely absent throughout.

Deconvoluted mass spectra revealed a complex picture of speciation in the presence of DTT (Fig. 2). At each level of DTT/protein tested, the major copper-bound species were CuCopAab and Cu_2CopAab (see Table 2). This suggests the presence of DTT drives the protein population towards a monomeric form with a fairly equal propensity for one or two copper-binding sites to be occupied. The ability of DTT to inhibit dimerisation may be due in part to its ability to compete well for Cu(I) bound by dimeric forms but less so with monomeric forms of CopAab. The affinity of DTT for Cu(I) ($K \sim 10^{15}$ M, [34]) is lower than that measured of the initial binding phase of CopAab ($K \sim 10^{17}$ M) [17], but higher than those modelled from spectroscopic data ($K \sim 10^5 – 10^9$) for binding of additional copper ions to CopAab.

At a 1:1 ratio of DTT to protein, in addition to the apo-, Cu and Cu_2CopAab forms observed in the absence of DTT, a Cu_4CopAab form was also observed, alone and as a DTT-adduct, along with a Cu_6CopAab$(DTT)_2$ adduct. Interestingly, the distribution of monomeric species remained relatively constant as the ratio of DTT to protein increased. Relative abundances of species (mean values over n = 3) are shown in Fig. S3. In all cases, DTT adducts involved the CopAab monomer binding 4 – 6 Cu(I) ions; no DTT adducts were observed for CopAab bound to 1 or 2 Cu(I). This suggests that DTT most likely plays an important role in directly binding Cu(I) in these complexes, effectively replacing

the Cys thiols that were provided by the second CopAab molecule in dimeric CopAab species, and enabling monomeric CopAab to bind significantly more Cu(I) than in the absence of DTT. The unexpected species Cu_4CopAab may represent a breakdown product of the Cu_4(CopAab:DTT) species. Interestingly, although DTT had a similar effect on the propensity of CopZ to dimerize in the presence of Cu(I), DTT complexes with CopZ were not observed by ESI-MS [22].

In the presence of BSH (1, 5, 10, 25/protein) the m/z spectra (Fig. S4) were significantly noisier, most likely reflecting ion suppression due to the presence of BSH, as previously observed for CopZ measurements [22]. CopAab peak envelopes were still detected, up to 25 BSH/protein, but beyond this level interpretation of the spectra was not possible (data not shown). The m/z spectra clearly contained three peak envelopes, due to monomeric (+8, +9) and two dimeric (+12 – 14; and +16 – 18) forms, as in the thiol-free spectrum (Fig 1D). The deconvoluted spectra, Fig. 3, remarkably show that in the presence of 1, 5 and 10 BSH/CopAab, there was a significant increase in the dimeric forms of CopAab relative to monomeric forms (see Table 2 for observed and predicted masses).

Dimeric species included $Cu_5(CopAab)_2$ and $Cu_6(CopAab)_2$, but also featured a previously undetected $Cu_7(CopAab)_2$ form, as well as a BSH adduct of $Cu_6(CopAab)_2$ ($Cu_6(CopAab)_2(BSH)$). At higher levels of BSH (25 BSH/CopAab), the relative proportion of dimeric form eventually decreased, but were still observed (Fig. 3D). Relative abundances of species (mean values over n = 3) are shown in Fig. S5. Significantly higher ratios of BSH:CopAab could not be investigated due to ion suppression [22].

The measured affinities for initial binding of Cu(I) to CopAab and BSH are similar ($K \sim 10^{17}$ M) [16, 22], which supports the observation of monomeric species in the presence of BSH, and increased abundance of monomeric CopAab at higher BSH levels. Although relatively few BSH adducts were detected (only $Cu_6(CopAab)_2(BSH)$ at 1 – 10 BSH/protein and possibly $Cu_5(CopAab)_2(BSH)$ at 25 BSH/protein), BSH clearly has a significant effect on Cu(I)-binding, leading to a distinct distribution of species observed in the presence of BSH, with CopAab dimeric forms detected containing between 5 to 7 Cu(I) ions, rather than between 4 to 6 Cu(I) in the absence of

BSH. This additional Cu(I)-binding and increased abundance of CopAab dimeric peaks suggests BSH may increase the copper-binding capacity by acting as an additional Cu(I) ligand; however, the general lack of BSH adducts means that this is unclear. We note that this is in stark contrast to CopZ, for which multiple BSH adducts were readily detected [22]. This may point to different roles *in vivo* for BSH with respect to formation of bacillithiolated species and to participation/cooperation in Cu(I)-binding by CopA N-terminal copper-binding domains and the chaperone CopZ. The concentration of BSH varies during growth, but is generally in the millimolar range [35]. Concentrations of copper trafficking proteins in *B. subtilis* have not been determined, but under copper stress conditions (0.4 mM Cu in growth media), total Cu reaches millimolar levels [3]. A CopZ mutant was found to accumulate ~ 3-fold less total Cu, indicating that, under these conditions, a large proportion of Cu is associated with CopZ, suggesting that it reaches concentrations in the hundreds of micromolar range [3]. Given that *copZ* and *copA* are co-expressed under the control of the CsoR regulator, and are significantly upregulated under copper stress conditions [36], the ratios of thiol to protein employed here are likely to be in the physiological range, at least under copper stress conditions. Thus, data reported here and those from the previous study of CopZ are entirely consistent with an important role for BSH in copper speciation in the cytoplasm and its export out of the cell.

Concluding remarks

ESI-MS under non-denaturing conditions has provided high resolution information on CopAab assembly state and the precise nature of Cu(I)-bound species. Monomeric CuCopAab and Cu_2CopAab are the main forms at levels of copper lower than 1/CopAab. Above this level, CopAab dimerization was observed, with the major dimeric species corresponding to $Cu_6(CopAab)_2$, with much smaller peaks due to $Cu_5(CopAab)_2$ and $Cu_4(CopAab)_2$ and no higher order copper bound forms, suggesting that $Cu_6(CopAab)_2$ is the most stable form of dimeric CopAab. The observation of two distinct dimeric charge state envelopes indicated the presence of distinct conformations that may be related

to previous observations of loss of secondary structure at higher copper loadings. The physiological importance of CopAab dimerization and Cu(I)-mediated unfolding is unclear, but one possibility is that this serves some kind of regulatory function perhaps through modulating interactions with transmembrane domains. While any such regulatory role in CopA remains to be demonstrated, we note that formation of a Cu(I)-transporting P-type ATPase (ATP7B, the Wilson disease protein) dimer was recently reported *in vitro* and in cells [29].

The influence of low molecular weight thiols on CopAab species distribution at elevated copper loadings (4 Cu/protein) was investigated and this confirmed that DTT efficiently inhibited CopAab dimer formation, and led to DTT adducts of CopAab, in which DTT most likely provides additional coordinating thiolate ligands that enable the formation of monomeric forms of CopAab capable of binding multiple Cu(I) ions, e.g., Cu_6CopAab$(DTT)_2$. In contrast, BSH was found to promote the formation of dimeric CopAab relative to monomeric forms, at least up to 10 BSH/CopAab. Species detected included $Cu_5(CopAab)_2$ and $Cu_6(CopAab)_2$, but also $Cu_7(CopAab)_2$, which was not detected in the absence of BSH, as well as the BSH adduct $Cu_6(CopAab)_2$(BSH). The data are consistent with BSH playing an important role in copper trafficking in *B. subtilis*.

Table of abbreviations

AUC	analytical ultracentrifugation
BSH	bacillithiol
CD	circular dichroism
CV	column volume
ESI-MS	electrospray ionisation mass spectrometry
DTT	dithiothreitol
HEPES	4-(2-hydroxyethyl)-1-piperazineethanesulfonic acid

NMR	nuclear magnetic resonance
MBD	metal-binding domain
SEC	size exclusion chromatography
SDS-PAGE	sodium dodecyl sulfate-polyacrylamide gel electrophoresis

Acknowledgements

We thank UEA for funding the purchase of the mass spectrometer used in this work, and for the award of a PhD studentship to KK.

References

[1] T.D. Rae, P.J. Schmidt, R.A. Pufahl, V.C. Culotta, T.V. O'Halloran, Science 284 (1999) 805-808.

[2] L. Banci, I. Bertini, S. Ciofi-Baffoni, M. D'Onofrio, L. Gonnelli, F.C. Marhuenda-Egea, F.J. Ruiz-Duenas, J. Mol. Biol. 317 (2002) 415-429.

[3] D.S. Radford, M.A. Kihlken, G.P.M. Borrelly, C.R. Harwood, N.E. Le Brun, J.S. Cavet, FEMS Microbiol. Lett. 220 (2003) 105-112.

[4] A.C. Rosenzweig, J.M. Arguello, Curr. Top. Membr. 69 (2012) 113-136.

[5] J.M. Arguello, J. Membr. Biol. 195 (2003) 93-108.

[6] F. Arnesano, L. Banci, I. Bertini, A.M.J.J. Bonvin, Structure 12 (2004) 669-676.

[7] J.R. Forbes, G. Hsi, D.W. Cox, J. Biol. Chem. 274 (1999) 12408-12413.

[8] I. Morin, S. Gudin, E. Mintz, M. Cuillel, FEBS J. 276 (2009) 4483-4495.

[9] M. Gonzalez-Guerrero, J.M. Arguello, Proc. Natl. Acad. Sci. U. S. A. 105 (2008) 5992-5997.

[10] M. Gonzalez-Guerrero, D. Hong, J.M. Arguello, J. Biol. Chem. 284 (2009) 20804-20811.

[11] C.C. Wu, W.J. Rice, D.L. Stokes, Structure 16 (2008) 976-985.

[12] N.M. Hasan, A. Gupta, E. Polishchuk, C.H. Yu, R. Polishchuk, O.Y. Dmitriev, S. Lutsenko, J. Biol. Chem. 287 (2012) 36041-36050.

[13] L.T. Braiterman, A. Gupta, R. Chaerkady, R.N. Cole, A.L. Hubbard, J. Biol. Chem. 290 (2015) 8803-8819.

[14] L. Zhou, C. Singleton, O. Hecht, G.R. Moore, N.E. Le Brun, FEBS J. 279 (2012) 285-298.

[15] L. Zhou, C. Singleton, N.E. Le Brun, Dalton Trans. 41 (2012) 5939-5948.

[16] C. Singleton, L. Banci, S. Ciofi-Baffoni, L. Tenori, M.A. Kihlkenl, R. Boetzel, N.E. Le Brun, Biochem. J. 411 (2008) 571-579.

[17] C. Singleton, N.E. Le Brun, Dalton Trans. (2009) 688-696.

[18] L. Zhou, K.L. Kay, O. Hecht, G.R. Moore, N.E. Le Brun, Biochim. Biophys. Acta 1866 (2018) 275-282.

[19] E.B. Maryon, S.A. Molloy, J.H. Kaplan, Am. J. Physiol. Cell Physiol. 304 (2013) C768-779.

[20] B.K. Chi, A.A. Roberts, T.T. Huyen, K. Basell, D. Becher, D. Albrecht, C.J. Hamilton, H. Antelmann, Antioxid. Redox Signal. 18 (2013) 1273-1295.

[21] Z. Rosario-Cruz, J.M. Boyd, Curr. Genet. 62 (2016) 59-65.

[22] K.L. Kay, C.J. Hamilton, N.E. Le Brun, Metallomics 8 (2016) 709-719.

[23] S.V. Sharma, V.K. Jothivasan, G.L. Newton, H. Upton, J.I. Wakabayashi, M.G. Kane, A.A. Roberts, M. Rawat, J.J. La Clair, C.J. Hamilton, Angew. Chem. Int. Ed. 50 (2011) 7101-7104.

[24] J.C. Crack, A.J. Thomson, N.E. Le Brun, Proc. Natl. Acad. Sci. U. S. A. 114 (2017) E3215-E3223.

[25] D.E. Sutherland, K.L. Summers, M.J. Stillman, Biochem. Biophys. Res. Commun. 426 (2012) 601-607.

[26] K.L. Kay, L. Zhou, L. Tenori, J.M. Bradley, C. Singleton, M.A. Kihlken, S. Ciofi-Baffoni, N.E. Le Brun, Chem. Commun. 53 (2017) 1397-1400.

[27] A. Volbeda, E.L. Dodd, C. Darnault, J.C. Crack, O. Renoux, M.I. Hutchings, N.E. Le Brun, J.C. Fontecilla-Camps, Nat. Commun. 8 (2017) 15052.

[28] T. Heitkamp, R. Kalinowski, B. Bottcher, M. Borsch, K. Altendorf, J.C. Greie, Biochemistry 47 (2008) 3564-3575.

[29] S. Jayakanthan, L.T. Braiterman, N.M. Hasan, V.M. Unger, S. Lutsenko, J. Biol. Chem. 292 (2017) 18760-18774.

[30] R.C. Fahey, Biochim. Biophys. Acta 1830 (2013) 3182-3198.

[31] Z. Ma, P. Chandrangsu, T.C. Helmann, A. Romsang, A. Gaballa, J.D. Helmann, Mol. Microbiol. 94 (2014) 756-770.

[32] Z. Fang, P.C. Dos Santos, Microbiologyopen 4 (2015) 616-631.

[33] G.L. Newton, M. Rawat, J.J. La Clair, V.K. Jothivasan, T. Budiarto, C.J. Hamilton, A. Claiborne, J.D. Helmann, R.C. Fahey, Nat. Chem. Biol. 5 (2009) 625-627.

[34] Z. Xiao, J. Brose, S. Schimo, S.M. Ackland, S. La Fontaine, A.G. Wedd, J. Biol. Chem. 286 (2011) 11047-11055.

[35] S.V. Sharma, M. Arbach, A.A. Roberts, C.J. Macdonald, M. Groom, C.J. Hamilton, Chembiochem 14 (2013) 2160-2168.

[36] G.T. Smaldone, J.D. Helmann, Microbiol. 153 (2007) 4123-4128.

Table 1. Observed and predicted masses of CopAab with variable copper loadings detected by ESI-MS.

CopAab with variable Cu in absence of low molecular weight thiol					
Species	**Predicted mass (Da)**	**Observed masses (Da)**			
		0.5 Cu/CopAab	**1.0 Cu/CopAab**	**2.0 Cu/CopAab**	**4.0 Cu/CopAab**
CopAab	15913	15911	15908	15908	15908
CuCopAab	15976	15975	15974	15973	15973
Cu_2CopAab	16038	16038	16038	16037	16038
$Cu_3(CopAab)_2$	32014	–	–	–	–
$Cu_4(CopAab)_2$	32076	–	–	32073	32071
$Cu_5(CopAab)_2$	32139	–	32139	32139	32140
$Cu_6(CopAab)_2$	32201	–	32201	32201	32202

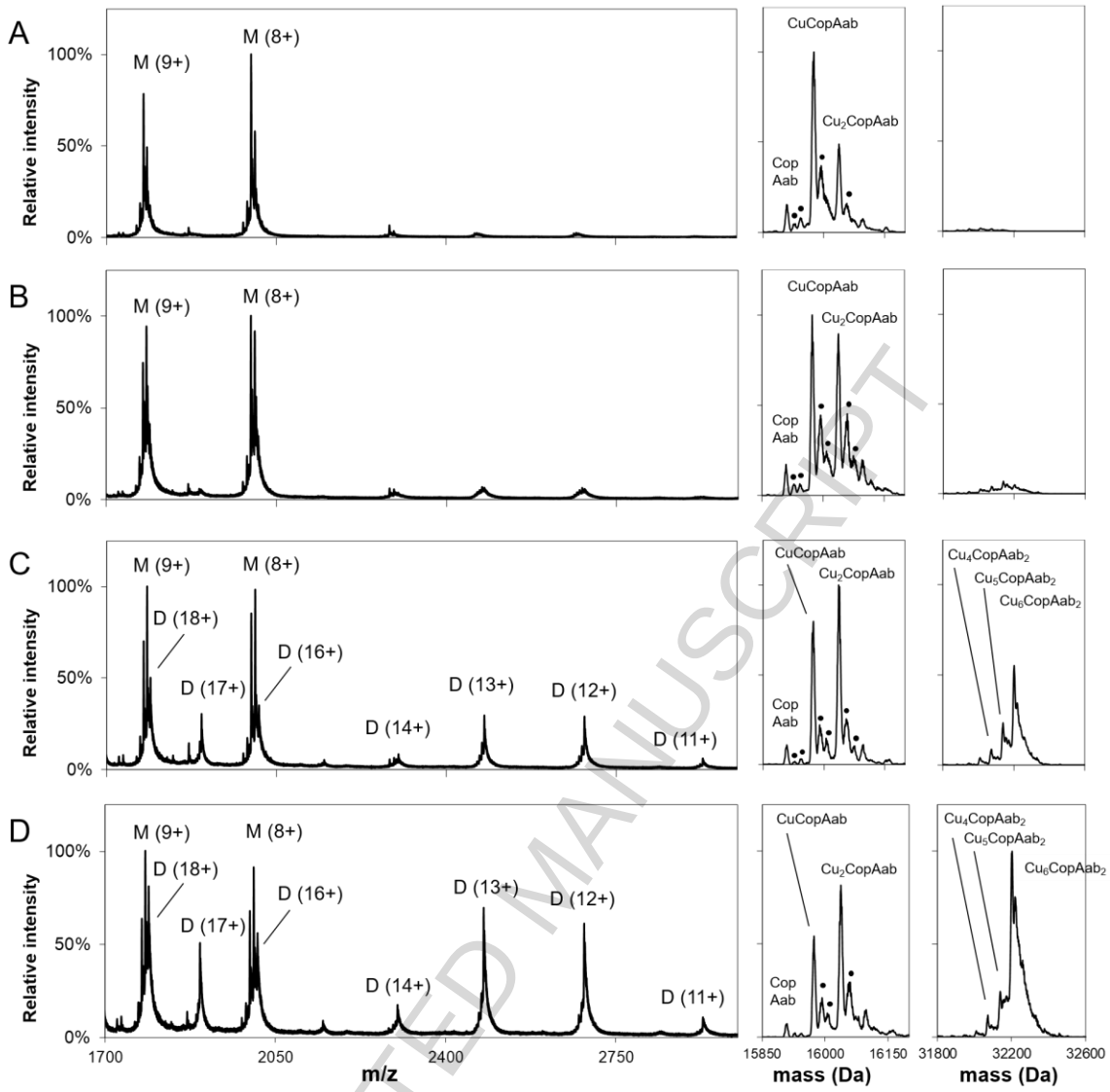

Figure 1. m/z mass spectra reveal two dimeric forms of CopAab. The mass spectra prior to, and after, deconvolution of CopAab reconstituted with Cu(I) at: **A)** 0.5 Cu / protein, **B)** 1 Cu / protein, **C)** 2 Cu / protein, **D)** 4 Cu / protein. (•) = sodium adduct. CopAab (5 µM) was in 20 mM ammonium acetate.

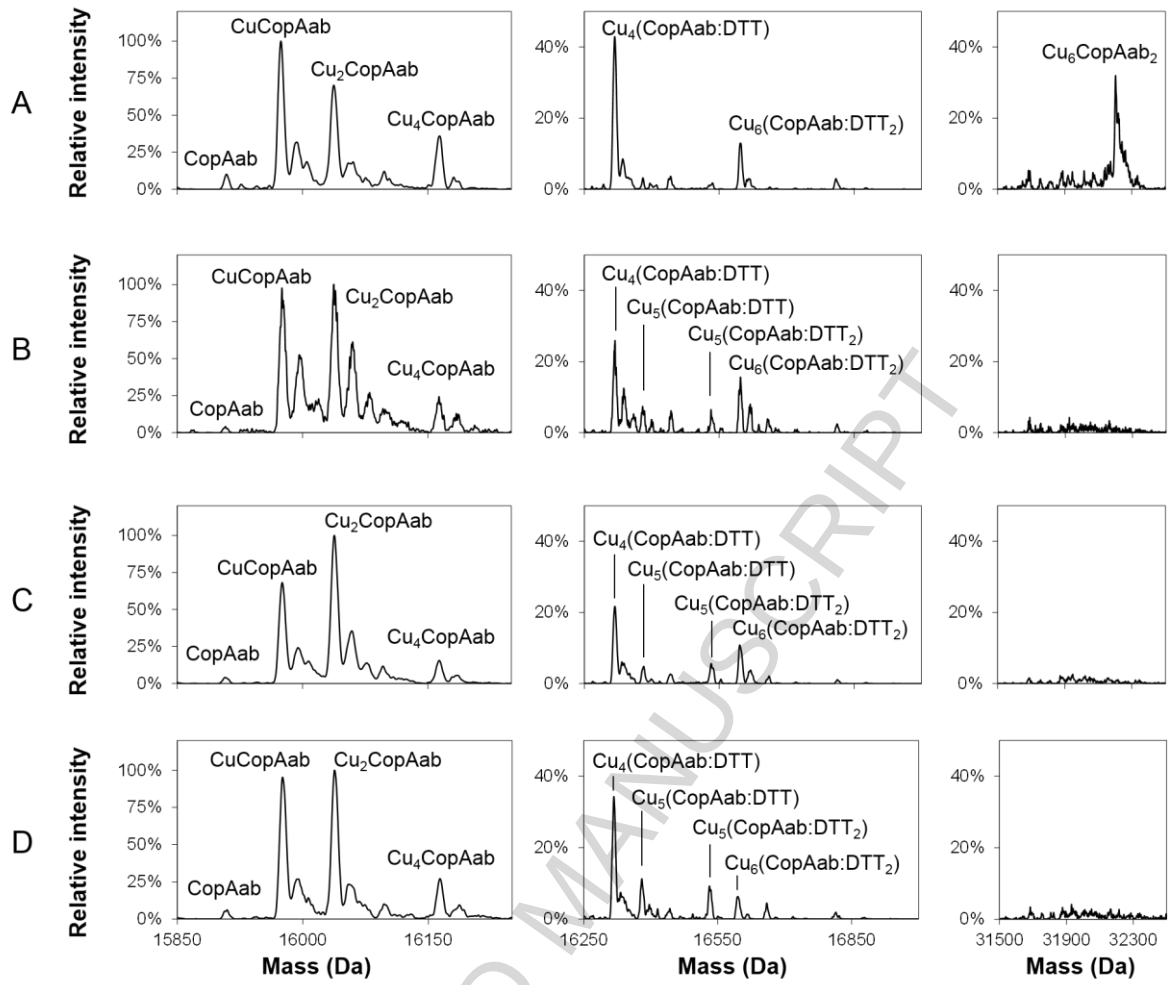

Figure 2. Deconvoluted mass spectra for 4 Cu/CopAab at increasing levels of DTT. Mass spectra of 4 Cu / CopAab in the presence of: **A)** 1 DTT / protein, **B)** 5 DTT / protein, **C)** 10 DTT / protein, **D)** 25 DTT / protein. The regions of the mass spectra, from left to right, are: CopAab monomer, DTT adducts of CopAab monomer, and CopAab dimer.

Table 2. Observed and predicted masses of ESI-MS detected CopAab in the presence of 4 Cu(I) per protein and variable low molecular weight thiols.

Species	**Predicted mass (Da)**	**Observed mass (Da)**			
4 Cu/CopAab in presence of variable DTT					
		1 DTT / CopAab	**5 DTT / CopAab**	**10 DTT / CopAab**	**25 DTT / CopAab**
CopAab	15913	15909	–	15908	–
CuCopAab	15976	15974	15976	15976	15976
Cu_2CopAab	16038	16037	16038	16038	16038
Cu_3CopAab	16101	16098	–	–	16100
Cu_4CopAab	16163	16164	16163	16164	16164
Cu_4(CopAab:DTT)	16317	16318	16317	16318	16317
Cu_5(CopAab:DTT)	16380	–	16383	16382	16380
Cu_5(CopAab:DTT)$_2$	16534	–	16532	–	16534
Cu_6(CopAab:DTT)	16442	–	16443	16444	–
Cu_6(CopAab:DTT)$_2$	16597	16597	16597	16599	16596
Cu_4(CopAab)$_2$	32076	32072	–	–	–
Cu_5(CopAab)$_2$	32139	32136	–	–	–
Cu_6(CopAab)$_2$	32201	32202	–	–	–
4 Cu/CopAab in presence of variable BSH					
		1 BSH / CopAab	**5 BSH / CopAab**	**10 BSH / CopAab**	**25 BSH / CopAab**
CopAab	15913	15909	15909	15909	15910
CuCopAab	15976	15975	15973	15973	15974
Cu_2CopAab	16038	–	–	–	–
Cu_3CopAab	16101	–	–	–	16100
Cu_4CopAab	16163	16163	16163	16163	16165
Cu_4(CopAab)$_2$	32076	–	–	–	32074
Cu_5(CopAab)$_2$	32139	32137	32135	32138	–
Cu_6(CopAab)$_2$	32201	32203	32203	32201	32202

$Cu_7(CopAab)_2$	32264	32265	32264	32266	32264
$Cu_8(CopAab)_2$	32326	32326	32325	32329	–
$Cu_5(CopAab)_2(BSH)$	32692	–	–	–	32693
$Cu_6(CopAab)_2(BSH)$	32756	32745	32746	32745	32753

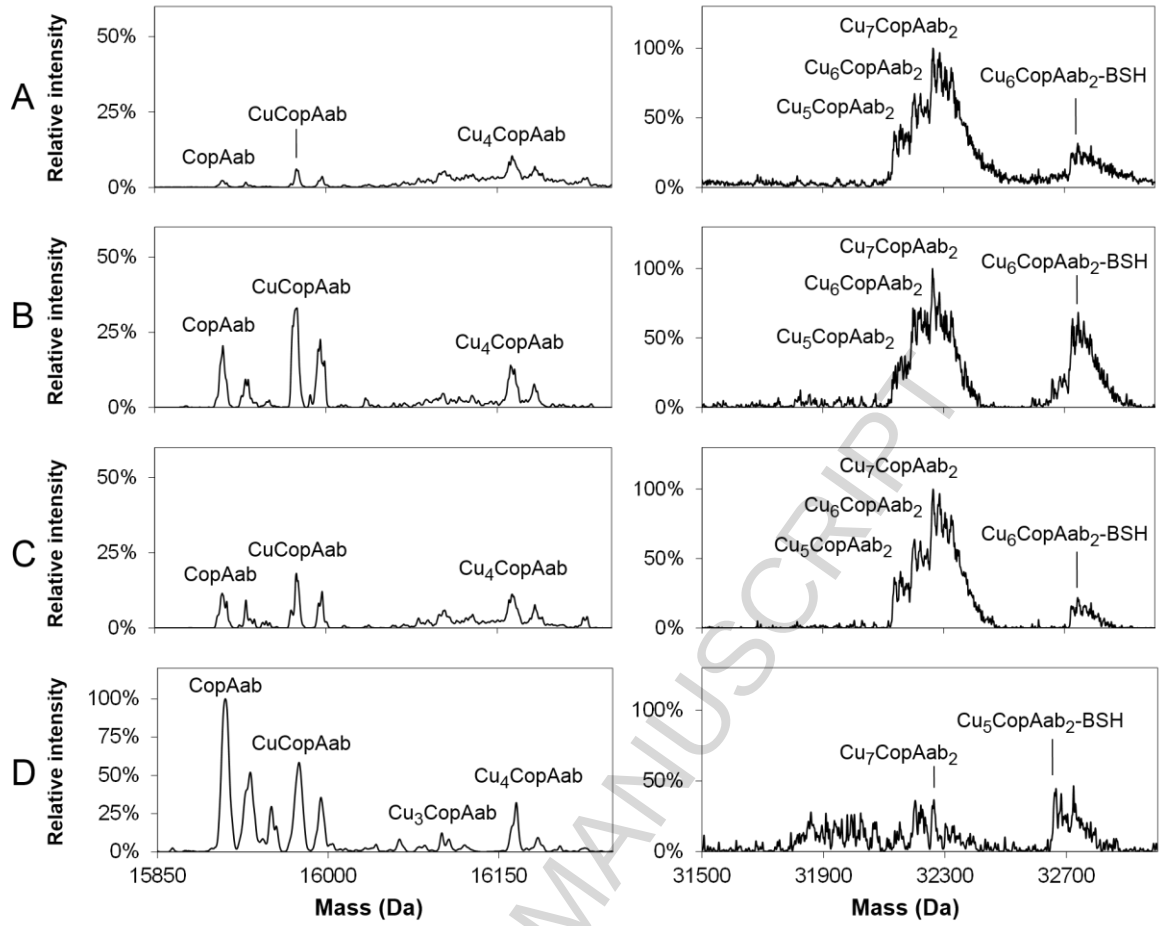

Figure 3. Deconvoluted mass spectra for 4 Cu/CopAab at increasing BSH levels. The deconvoluted mass spectra of 4 Cu / CopAab in the presence of: A) 1 BSH / protein, B) 5 BSH / protein, C) 10 BSH / protein, D) 25 BSH / protein.